



# Fabrication and Characterization of Titanium Dioxide (TiO<sub>2</sub>) Nanorods and Nanoflowers on Fluorine Doped Tin Oxide (FTO) for Ethanol Gas Sensor Application

Nurul Amiera Shahida Maarof<sup>1,2</sup>, Mohd Khairul Ahmad<sup>1,2\*</sup>, Soon Chin Fhong<sup>1,2</sup>, Syafa Syahirah Taib<sup>2</sup>, Nurhayati Muhd Ramli<sup>2</sup>, Nafarizal Nayan<sup>1,2</sup>, Mohamad Hafiz Mamat<sup>3</sup>, Suriani Abu Bakar<sup>4</sup>, Azmi Mohamed<sup>4</sup> and Masaru Shimomura<sup>5</sup>

<sup>1</sup>Faculty of Electrical & Electronic Engineering, Universiti Tun Hussein Onn Malaysia, 86400 Parit Raja, Batu Pahat, Johor, Malaysia, nurulamierashahidamaarof96@gmail.com, akhairul@uthm.edu.my, soon@uthm.edu.my, nafa@uthm.edu.my,

<sup>2</sup>Microelectronics & Nanotechnology Shamsuddin Research Centre, Universiti Tun Hussein Onn Malaysia, 86400 Parit Raja, Batu Pahat, Johor, Malaysia, syafa501@gmail.com, nurhayatimuhdramli@gmail.com,

<sup>3</sup>NANO-ElecTronic Centre (NET), Faculty of Electrical Engineering, Universiti Teknologi MARA, 40450, Shah Alam, Selangor, Malaysia, mhmamat@uitm.edu.my,

<sup>4</sup>Nanotechnology Research Centre, Faculty of Science and Mathematics, Universiti Pendidikan Sultan Idris, 35900, Tg. Malim, Perak, Malaysia, absurdiani@yahoo.com, azmi.mohamed@fsmt.ups.edu,

<sup>5</sup>Department of Engineering, Graduate School of Integrated Science and Technology, Shizuoka University, 432-8011 Hamamatsu, Shizuoka, Japan, shimomura.masaru@shizuoka.ac.jp.

## ABSTRACT

Titanium dioxide (TiO<sub>2</sub>) is one of the metal oxide semiconductor materials. In this study, TiO<sub>2</sub> nanorods and nanoflowers were deposited using a hydrothermal method at constant temperature (150 °C) on top of fluorine doped tin oxide (FTO) substrate. The hydrothermal reaction times were varied to 8, 12, 16, 20 and 24 hours. The morphological and structural properties of the samples were characterized by using Electron Microscopy (FESEM) and X-ray Diffraction (XRD), respectively. The optimized samples of TiO<sub>2</sub> nanorods and nanoflowers were 8 and 16 hours respectively due to has the highest crystallinity among others since it recorded the lowest full width at half maximum (FWHM) values. During the gas sensing measurement, the samples were heated at 200 °C and exposed to ethanol vapor, then the current changes were recorded. From the result obtained, TiO<sub>2</sub> nanorods based ethanol gas sensor recorded the lowest value of sheet resistance because it provided a better electron flow on the device. Meanwhile, it also has the highest value of conductivity compared to TiO<sub>2</sub> nanoflowers based device.

**Key words:** Ethanol gas sensor, hydrothermal, nanoflowers, nanorods, TiO<sub>2</sub>

## 1. INTRODUCTION

Gas sensors play an essential role, especially in term of environment monitoring and chemical process controlling. Gas sensors play an important role, especially in term of

environment monitoring and chemical process controlling [1]. For the recent years, metal oxide-based sensors have been briefly studied due to has various of advantages which are low-cost production of material, a wide range of detectable gasses and has an easy setup production [2] - [5]. There are several types of gas sensors which includes organic compounds gas sensors [6], solid electrolyte gas sensors [7], electrochemical gas sensors [8], graphene-based gas sensors [9] and metal oxide gas sensors [10] - [11]. The metal oxide-based gas sensor consists of metal oxide semiconductors material such as zinc oxide (ZnO), nickel oxide (NiO), copper oxide (CuO), tin dioxide (SnO<sub>2</sub>), iron (III) oxide (Fe<sub>2</sub>O<sub>3</sub>) and titanium dioxide (TiO<sub>2</sub>) [13] - [15]. Due to the interaction between the gas molecule and the surface of the nanostructures, an interchange of trapping of free carriers will be produced, which explained the gas sensing mechanism.

TiO<sub>2</sub> nanotubes arrays have been successfully fabricated by using the anodic oxidation process with a highly ordered structural and controllable size of nanotubes for ethanol gas sensor application [16]. The morphological and the structural properties of the TiO<sub>2</sub> nanotubes were studied by using FESEM, TEM and XRD. The gold (Au) contact has been used as the working electrode. The sensing measurement was measured in the sealed chamber, and the device was heated at 250 °C. During measurement, ethanol was injected into the testing tube by using microsyringe to obtain ethanol concentration of 50-1000ppm, the electrical current in the nanotubes was measured. The current increased rapidly when

the sensor exposed to ethanol gas then recovered to the initial value thoroughly when the sensor introduced to the air. According to the dynamic responses of TiO<sub>2</sub> nanotubes gas sensor, the sensor showed a little bit unstable response to 50 ppm while showed a very stable response towards 1000 ppm. These showed that the sensor was insensitive towards a lower concentration of ethanol gas [16].

Other than that, [15] had excellently fabricated TiO<sub>2</sub> nanostructures metal-semiconductor-metal (MSM) humidity sensor on top of p-type silicon substrates by using chemical bath deposition (CBD) method. The characterization of the structures was made by using FESEM, XRD, EDX and RAMAN. Instead of using a gold electrode, platinum (Pt) electrode was used as the electrode and deposited by using RF reactive magnetron sputtering method with the thickness of 100 nm. The current-voltage (I-V) characteristics of the device was measured in environmental humidity of 70% at room temperature. The I-V characteristic does not have the same values at different relative humidity (RH) value, while the conductance of the device was directly proportional to RH concentration. The efficiency of the resistivity and the response of the sensor will be enhanced by having a high surface/volume ratio. The physisorption phenomena will be occurred at room temperature due to the interaction between the molecules in water and semiconductor surface [15].

Meanwhile, [13] has been fabricated TiO<sub>2</sub> nanorods gas sensor on top of the FTO substrate by using a hydrothermal method for 18 hours of hydrothermal reaction time at 150 °C. The characterization of TiO<sub>2</sub> nanorods was focused on the morphological and structural properties studied by using FESEM and XRD. The fabricated thin film then was deposited with gold as the electrode by using a thermal evaporation system, and the thickness of the gold contact is 150 nm. The sensing measurement took place in a homemade chamber with the device heated at a constant temperature of 200 °C until obtains the steady state under high purify of dry air. The changes in DC current against time was recorded when the device exposed to 250-2000 ppm of H<sub>2</sub> while another volatile organic compound (VOC) materials at 5000 ppm. When the device was exposed to H<sub>2</sub> gas, the response increased due to the depletion surface layer decreases while the number of charge carriers which caused by the chemical reaction. During the gas sensing measurement with 5000 ppm of ethanol, isopropanol, methanol, chloroform, carbon tetrachloride (CCl<sub>4</sub>) and acetone, the device only able to sense isopropanol at high concentration [13]. These show that there is no response data of gas sensing measurement for over 1000 ppm of ethanol were recorded [17].

From these, TiO<sub>2</sub> has been extensively studied and considered as one of the most promising materials for the gas detection application. TiO<sub>2</sub> exists in three crystal form which are

anatase, brookite and rutile. As a metal oxide semiconductor material, TiO<sub>2</sub> has wide band-gap energy (~3.2 eV), high sensitivity, high stability, low cost and non-toxic material which does not harm to the environment [14], [18] – [21]. Other than that, TiO<sub>2</sub> has a high refractive index, and low adsorption coefficient is suitable for various applications such as anti-corrosion coating, solar cell, photocatalysis, lithium batteries, energy storage device and gas sensor [22], [18], [14]. Moreover, several TiO<sub>2</sub> nanostructures can be produced such as microspheres, nanowires, nanotubes, nanorods and nanoflowers [18], [19]. TiO<sub>2</sub> can be deposited by using a variety of methods such as chemical spray pyrolysis, RF magnetron sputtering, chemical vapor deposition, dip coating, sol-gel process, solvothermal, electrodeposition and hydrothermal method [18], [19], [23]. The solution-based method was a preferred method to fabricate nanostructures in producing high-quality TiO<sub>2</sub> as it is consuming low cost while allowing the fabrication of sensors at a minimal price. Besides that, the desired nanostructures can be obtained by controlling some parameters. The preferred material for gas sensors due to its low resistivity to the reduced driving power of the sensor [22]. Hence, TiO<sub>2</sub> nanostructures is a good choice for the fabrication of inexpensive and sensitive gas sensors.

Most of the existing gas sensor were fabricated by coating the sensing materials on the outer ceramic tube with electrodes and heaters [24]. From this method, the consistency and homogeneity of the sensor were not easy to preserve the excellent quality, especially in the industry. Besides, the existing sensor shows low sensitivity towards the gas during measurement. Hence, in this study, TiO<sub>2</sub> nanorods and nanoflowers based gas sensor were fabricated by using hydrothermal method on top of FTO substrate at various hydrothermal reaction time. Meanwhile, the structural and morphological properties of TiO<sub>2</sub> nanostructures were obtained from XRD and FESEM measurements. Thus, the findings regarding current-time (I-t) will be compared.

## 2. MATERIALS AND METHODS

The substrates were cleaned ultrasonically by using acetone, ethanol and DI water respectively for 5 minutes each and then dried in room temperature. The characteristic of the substrate was transparent, low cost, has high-temperature resistant and chemically inert [3]. The hydrothermal solution was prepared in a beaker that contained 120 mL of DI water and added 140 mL of HCl. The mixture was stirred vigorously, then 5 mL of TBOT was added dropwise into the solution using a plastic pipette. The solution transferred into a steel-lined Teflon autoclave where the substrates were placed. The FTO substrates were placed 45° vertically against the wall for the growth of nanorods. After nanorods had reached their growth limitation, and due to the gravitational forces, the nanoflowers will grow on top of the rods [25]. Hence as for the

growth of nanoflowers, the substrates were placed 180° which the conductive side is facing upward. The autoclave was placed in an electronic oven for 16 hours at a constant temperature of 150°C. After cooling down, TiO<sub>2</sub> samples were rinsed with DI water and dried at room temperature.

The surface morphology, cross-sectional area and the uniformity of the sample were analyzed by using FESEM (JEOL JSM-7600F) while the crystallinity of the structure was studied using XRD (PANalytical X-Pert<sup>3</sup> Powder). The optimize samples were deposited with 150 nm thickness of Au, 40 mA of plasma current while K is a constant that based on the material of metal and gas used in the experiment. K = 0.17 and, applied voltage, V constant at 1 kV.

The thickness can be obtained from equation (1). The Au contact acted as a metal contact and was deposited by using auto-fine coater machine. The illustration of the masking, as shown in Figure 1.

$$d = KIVt \tag{1}$$

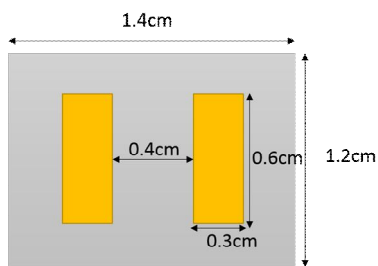


**Figure 1:** Illustration of the masking for gold contact on FTO substrate and the measurement details.

The sample of nanorods and nanoflowers were optimized from the result of FESEM and XRD. The devices were heated at 200 °C due to obtain steady state under high purify of dry air [13]. The devices were exposed to ethanol vapor, and the value of the concentration in parts-per-millions (ppm) was calculated. A constant voltage supplied from the source meter was -0.5V to 0.5V. The changes in (I-t) was recorded upon the exposure of the evaporated ethanol vapor to the devices. Figure 2 shows the illustration of arrangement during the gas measurement in the chamber.

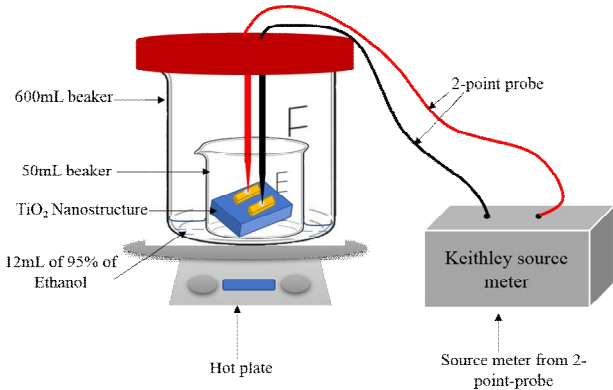


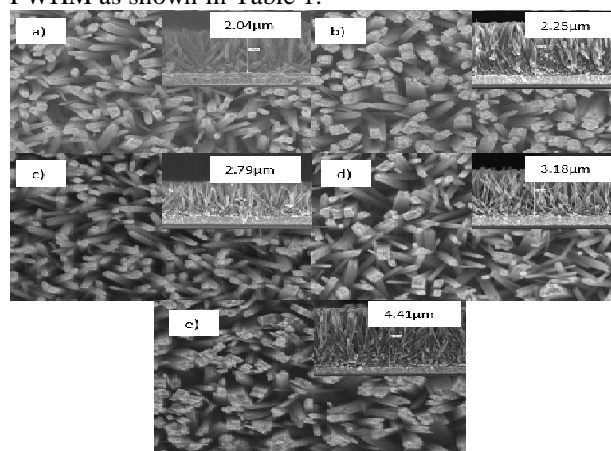
**Figure 2:** The illustration of the set up during the gas sensing measurement.

### 3. RESULTS AND DISCUSSIONS

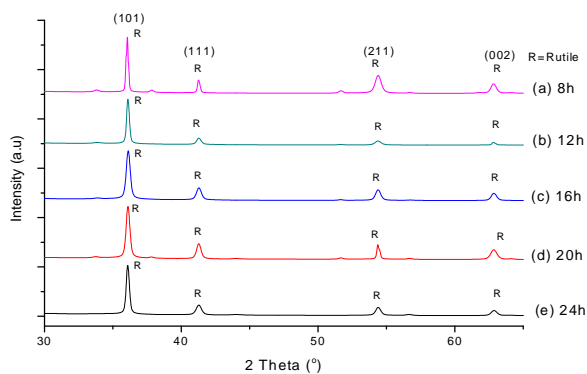
#### 3.1 Surface Morphology, Cross-Section Area and Crystalline Structure for TiO<sub>2</sub> Nanorods Arrays

Figure 3 shows the resulting images of TiO<sub>2</sub> nanorods arrays from FESEM measurement at different reaction times range from 8 until 24 hours. The result of the surface morphology and cross-section area for nanorods arrays, as shown in Figure 3 (a), (b), (c), (d) and (e). The nanorods were seen forming on top of the substrate perpendicularly with the thickness of the nanorods were 2.04 μm, 2.25 μm, 2.79 μm, 3.18 μm, 4.41 μm. The result showed that the thickness of TiO<sub>2</sub> nanorods will increase with the increasing of hydrothermal reaction time [19]. The crystallinity of TiO<sub>2</sub> nanorods arrays can be observed from XRD pattern obtained from XRD measurement as shown in Figure 4 (a), (b), (c), (d) and (e) which represents the patterns for different hydrothermal reaction times which are 8, 12, 16, 20 and 24 hours respectively. The dominant peaks of rutile TiO<sub>2</sub> in Figure 4 at 36°, 41° and 54° corresponding to the orientation plane of (101), (111) and (211) respectively. The highest intensity for rutile TiO<sub>2</sub> nanorods arrays among the others was centred at peak 36° at the plane (101), and this plane was considered as the preferred plane for TiO<sub>2</sub>. Since the thickness of nanorods arrays increases with the increasing of the reaction time, there are no FTO peaks recorded in the XRD pattern.

These proven by the surface morphology result from FESEM which the nanorods arrays were fully grown on top of the FTO surface and the gap between the rods were eliminated. Overall peaks from the result obtained shows that there is no broad peak produced which indicates that the characteristic of good crystallinity of the sample. All the peaks were compared with standard diffraction data of rutile-phased TiO<sub>2</sub> cited from the 1998 Joint Committee on Powder Diffraction Standards-International Centre for Diffraction Data (JCPDS). From the result obtained from FESEM and XRD, 8 hours of hydrothermal reaction times were chosen as it gives the highest crystallinity since it recorded the lowest value of FWHM as shown in Table 1.



**Figure 3:** The FESEM results of TiO<sub>2</sub> nanorods arrays surface morphology and cross-section area for (a) 8, (b) 12, (c) 16, (d) 20 and (e) 24 hours hydrothermal reaction time and the thickness of rods respectively.



**Figure 4:** The XRD patterns of TiO<sub>2</sub> nanorods arrays for (a) 8, (b) 12, (c) 16, (d) 20 and (e) 24 hours hydrothermal reaction time respectively and the rutile peaks were indexed to (101), (111), (211) and (002) diffraction peaks while R is referring to rutile phase.

### 3.2 Surface Morphology, Cross-Section Area and Crystalline Structure for TiO<sub>2</sub> Nanoflowers Arrays

TiO<sub>2</sub> nanoflowers arrays were prepared with the same parameters as the preparation of TiO<sub>2</sub> nanorods arrays. Figure 5 (a), (b), (c), (d) and (e) represented the result obtained from FESEM measurement of the morphology and cross-section area of the samples for 8, 12, 16, 20 and 24 hours of hydrothermal reaction time respectively. From Figure 5, the number of nanoflowers grew, and the thickness increases with the increasing of hydrothermal reaction time due to having sufficient reaction time to produce more TiO<sub>2</sub> nanoflowers. The thickness of the nanoflowers formed at 8, 12, 16, 20 and 24 hours were about 2.78 μm, 3.22 μm, 3.86 μm, 7.88 μm and 8.12 μm respectively.

Figure 6 (a), (b), (c), (d) and (e) indicates the result obtained from XRD measurement regarding the crystallinity of TiO<sub>2</sub> nanoflowers arrays for different hydrothermal reaction time. There were clear diffraction peaks were recorded in between 25° and 65°, which consists only rutile TiO<sub>2</sub> peaks. The dominant peaks of rutile TiO<sub>2</sub> nanoflowers arrays at 27°, 36° and 54° which corresponding to the orientation plane (110), (101) and (211) respectively. Since the thickness of nanoflowers arrays increases with the increase of reaction time, there is no FTO peak recorded in the XRD pattern. These have been proven with the result obtained from FESEM which the nanoflowers arrays were fully grown on top of the nanorods surfaces. Thus, the optimized sample obtained from this observation was 16 hours of hydrothermal reaction time as it gave the highest crystallinity since it recorded the lowest value of FWHM, as shown in Table 1.

**Table 1:** FWHM values for TiO<sub>2</sub> nanorods and nanoflowers.

Reaction time (hours)	FWHM	
	TiO <sub>2</sub> nanorods	TiO <sub>2</sub> nanoflowers
8	0.0984	0.1378
12	0.1968	0.0984
16	0.3149	0.0960
20	0.2952	0.3346
24	0.1440	0.2755

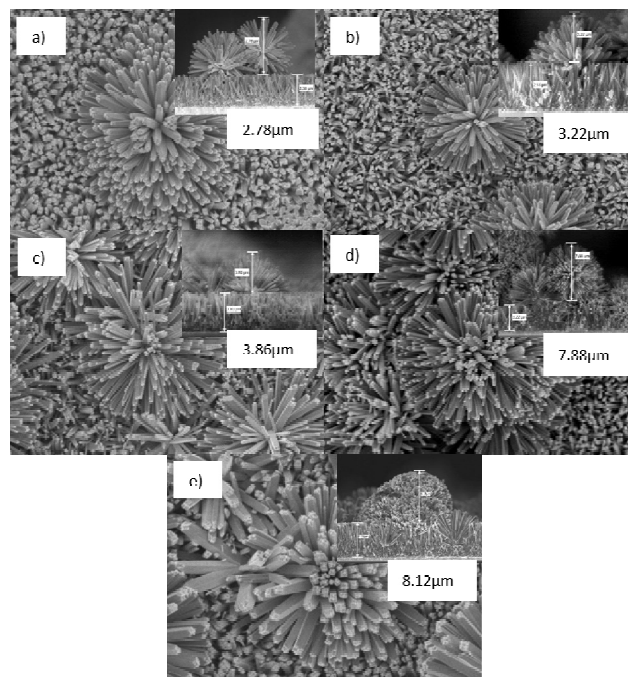


**Figure 5:** The FESEM results of TiO<sub>2</sub> nanoflowers arrays surface morphology and cross-section area for (a) 8, (b) 12, (c) 16, (d) 20 and (e) 24 hours hydrothermal reaction time and the thickness of the nanostructures respectively.

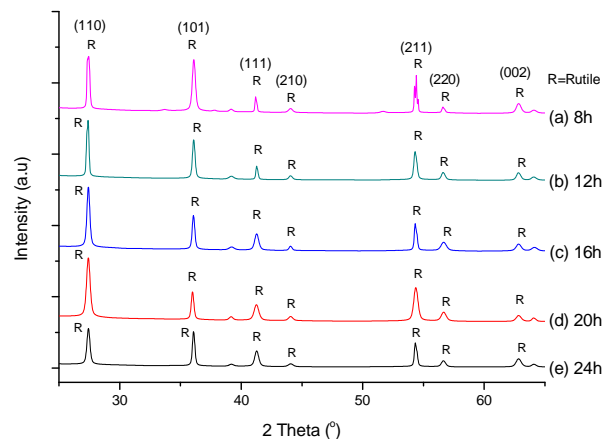


**Figure 6:** XRD patterns of TiO<sub>2</sub> nanoflowers arrays for (a) 8, (b) 12, (c) 16, (d) 20 and (e) 24 hours hydrothermal reaction time respectively and the rutile peaks were indexed to (110), (101) and (211) diffraction peaks while R is referring to rutile phase.

### 3.3 Ethanol Gas Sensor

In this study, the measurement took place by observing the current changes when the TiO<sub>2</sub> nanostructures-based device was exposed to the ethanol vapor. The time exposure of the vapor had an interval of two minutes, and the readings were recorded for 14 times for each session. When TiO<sub>2</sub> nanostructures exposed to certain gasses, the detection principle was needed during the process [26]. Moreover, if the

reaction between gas and nanostructures were strong or chemisorption, free-electron will transfer between the nanostructures while absorbed species will take place. Thus, there will be changes in charge carrier concentration and the conductivity of the material.

### 3.4 TiO<sub>2</sub> Nanorods Based Ethanol Gas Sensor

According to Figure 7, during the early exposure of ethanol vapor to the device, unstable response occurred and resulting low number of electrons transfer as well as low current recorded. When the exposure time exceeded 1400s, it recorded the highest peak among the others. These because the chamber already occupied with the ethanol vapor and the interaction between TiO<sub>2</sub> nanorods and the molecule in ethanol was the strongest. The other reason why it took a long time to reach the maximum interaction between them due to the surface morphological of TiO<sub>2</sub> itself. As a typical reductive gas, as the device exposed to ethanol vapor, it will react with the adsorbed oxygen species which lead to the release of the adsorb electron, e<sup>-</sup> [27]. The pre-existing oxygen ions on the surface of the TiO<sub>2</sub> nanostructure will react with the ethanol molecule, as shown in the illustration in Figure 8. The CO<sub>2</sub> and H<sub>2</sub>O were formed and the e<sup>-</sup> was released back to TiO<sub>2</sub> nanostructures. The summarization of the result obtained from the measurement shown in Table 2.

### 3.4 TiO<sub>2</sub> Nanoflowers Based Ethanol Gas Sensor

Compared to TiO<sub>2</sub> nanorods, TiO<sub>2</sub> nanoflowers have a different type of surface morphology and has higher detection surface for the interaction between ethanol molecule and TiO<sub>2</sub> nanoflowers. Upon the exposure of ethanol vapor to the device, it shows the highest peak of current recorded among others since there were many electrons transferred. As shown in Figure 9, after 700s of ethanol vapor exposure, the current decreases and started to be unstable after that. These because the O<sup>-</sup> ions produced during the process had fully covered and attached to the TiO<sub>2</sub> nanoflowers surface while the free electron still free transferred and experienced collision between each other. The illustration regarding the detection principle of ethanol molecule and TiO<sub>2</sub> nanoflowers, as shown in Figure 10. The obtained result was summarized in Table 2.

**Table 2:** The resistivity, conductivity, sheet resistance for TiO<sub>2</sub> nanorods and nanoflowers ethanol gas sensor device.

Resistivity, ρ (Ωcm)		Conductivity, σ (S/cm x 10 <sup>-3</sup> )		Sheet resistance, R <sub>s</sub> (Ω x 10 <sup>3</sup> )	
TiO <sub>2</sub> nanorods	TiO <sub>2</sub> nanoflowers	TiO <sub>2</sub> nanorods	TiO <sub>2</sub> nanoflowers	TiO <sub>2</sub> nanorods	TiO <sub>2</sub> nanoflowers
18.01	194.61	55.52	5.14	360.2	3.89

### 3.4 Summarization of Ethanol Gas Sensor

By comparison that has been made in Table 2, sheet resistance, R<sub>s</sub> is inversely proportional to conductivity, which is whenever the value of R<sub>s</sub> increases, there is dramatically decreased in value of conductivity, σ. The lower value of conductivity provided a better electron flow on the device [19]. From Table 2, TiO<sub>2</sub> nanorods based ethanol gas sensor recorded the lowest value of R<sub>s</sub>, which is 360.2 x 10<sup>3</sup> Ω compared to TiO<sub>2</sub> nanoflowers is 3.89 x 10<sup>6</sup> Ω. These proved that electron flows at the highest amount on the device. Hence, the conductivity of TiO<sub>2</sub> nanorods had the highest value, which is 55.52 x 10<sup>-3</sup> S/cm while 5.14 x 10<sup>-3</sup> S/cm for TiO<sub>2</sub> nanoflowers. These showed that TiO<sub>2</sub> nanorods device was the optimum device for gas sensing materials because it has the highest conductivity since conductivity is the vital factor in gas sensing.

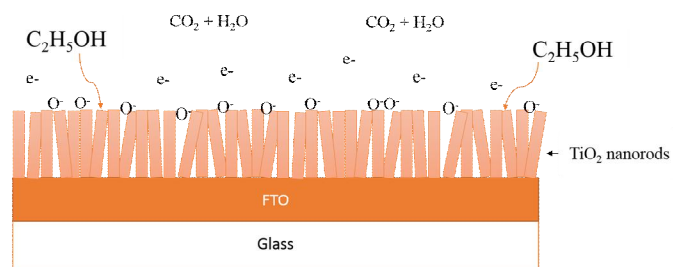


**Figure 8:** Illustration of the detection mechanism of TiO<sub>2</sub> nanorods with ethanol molecule.

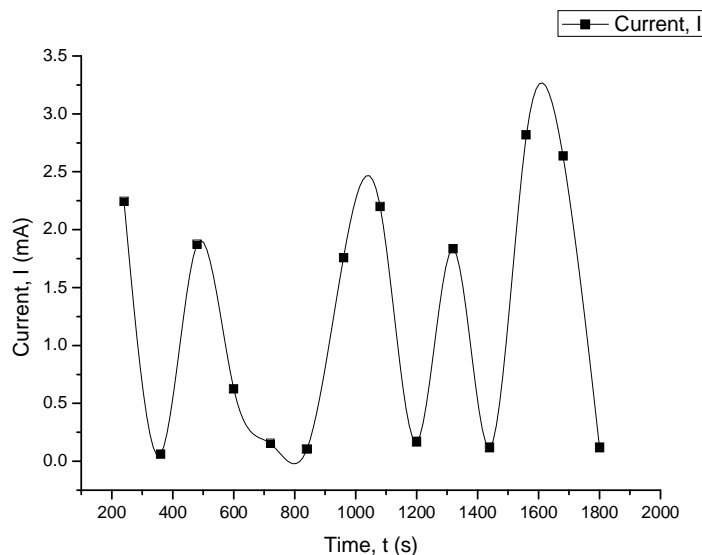


**Figure 7:** Graph current-time (I-t) for TiO<sub>2</sub> nanorods based ethanol gas sensor device.

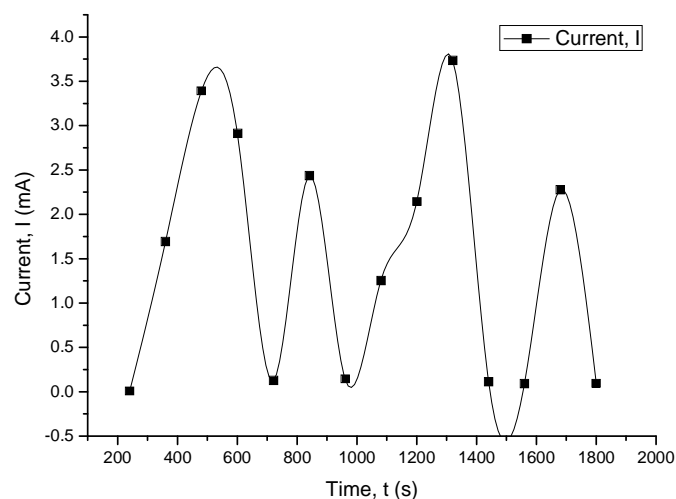


**Figure 9:** Graph current-time (I-t) for TiO<sub>2</sub> nanoflowers based ethanol gas sensor device.

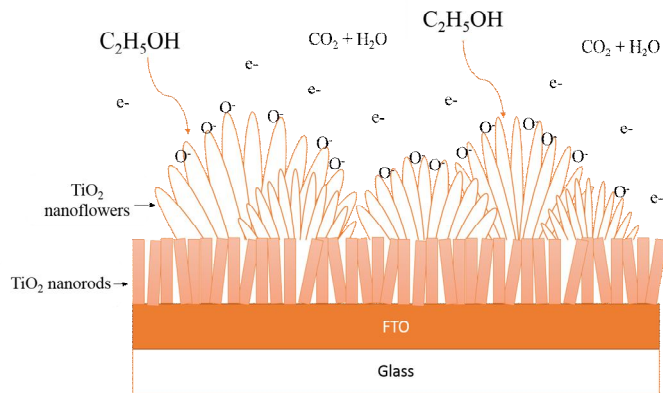


**Figure 10:** Illustration of the detection mechanism of TiO<sub>2</sub> nanoflowers with ethanol molecule.

#### 4. CONCLUSIONS

Rutile titanium dioxide (TiO<sub>2</sub>) nanorods and nanoflowers were successfully fabricated on top of fluorine doped tin oxide (FTO) substrate by using the hydrothermal process at a constant temperature of 150 °C. TiO<sub>2</sub> solution was prepared using 140 mL of hydrochloric acid (HCl), 120 mL of deionized (DI) and 5 mL of titanium butoxide as the precursor. At the same time, the hydrothermal reaction time was varied to 8, 12, 16, 20 and 24 hours. The characterization of TiO<sub>2</sub> nanorods and nanoflowers were made by using FESEM and XRD, and the optimized samples were 8 and 16 hours of hydrothermal reaction time for TiO<sub>2</sub> nanorods and nanoflowers, respectively. TiO<sub>2</sub> nanorods based device was the optimum device since it has the highest conductivity compared to TiO<sub>2</sub> nanoflowers based device.

Other than conductivity aspect, the sensitivity of the ethanol molecule with TiO<sub>2</sub> nanostructures. In this study, the ethanol gas sensor was fabricated by using undoped rutile TiO<sub>2</sub> nanostructures. Thus, it shows less sensitivity toward ethanol vapour. To enhance the sensitivity during sensing measurement, an addition of dopants such as Nb, Cr, Sn, Pt,

Zn, Al, Ag, La and Y were needed. The device that has been modified (doped TiO<sub>2</sub>) showed higher sensitivity compared to the unmodified (undoped TiO<sub>2</sub>) device. Other than that, activation energy such as heating at a higher temperature (300 °C – 500 °C) and exposed the device to UV light is needed to increase the sensitivity towards the gas [26]. Otherwise, the response towards the gas become slow, or there will be no response recorded.

#### ACKNOWLEDGEMENT

This work has been supported by the Geran Penyelidikan Pascasiswazah (GPPS) Vot. H570 and Multi-Disciplinary Research Grant (MDR) Vot. H471 from Universiti Tun Hussein Onn Malaysia, Ministry of Higher Education Malaysia.

#### REFERENCES

1. T. Mudgal, A. Rani, M. Dwivedi, T. Dadhich, A. Balraj, V. Prakash, A.K. Sharma, J. Bhargava and G. Eranna, **Optimization of sensor temperature for sensing ethanol gas using titanium oxide films.**
2. N. Barsan, D. Koziej and U. Weimar. **Metal oxide-based gas sensor research: How to?** *Sensors and Actuators B: Chemical*, vol. 121, no. 1, pp. 18–35. Jan 2007.
3. R. S. Devan, R. A. Patil, J. H. Lin and Y. R. Ma. **One-dimensional metal-oxide nanostructures: recent development in synthesis, characterization, and applications.** *Advanced Functional Materials*, vol. 22, no. 16, pp. 3326–3370. Aug 2012.
4. G. Sberveglieri, C. Baratto, E. Comini, G. Faglia, M. Fer-roni, A. Ponzoni and A. Vomiero. **Synthesis and characterization of semiconducting nanowires for gas sensing.** *Sensors and Actuators B: Chemical*, vol. 121, no. 1, pp. 208–213. Jan 2007
5. C. Wang, L. Yin, L. Zhang, D. Xiang and R. Gao. **Metal oxide gas sensors: Sensitivity and influencing factors.** *Sensors*, vol. 10, no. 3, pp. 2088–2106. Mar 2010.
6. . Yan, C. Wladyka, J. Fujii, and S. Sockanathan. **Prdx4 is a compartment-specific H<sub>2</sub>O<sub>2</sub> sensor that regulates neurogenesis by controlling surface expression of GDE2.** *Nature Communications*. vol. 6, no. 1, pp. 1-12, May 2015.
7. N. Miura, M. Nakatou and S. Zhuiykov. **Impedancetric Gas Sensor Based on Zirconia Solid Electrolyte and Oxide Sensing Electrode for Detecting Total NO<sub>x</sub> at High Temperature.** *Sensors and Actuators B: Chemical*, vol. 93, no. 1-3, pp. 221–228, August 2003.
8. W. Weppner. **Solid-state electrochemical gas sensors.** *Sensors and Actuators*, vol. 12, no. 2, pp. 107–119, Aug 1987.
9. G. Kulkarni, K. Reddy, Z. Zhong and X. Fan. **Graphene nanoelectronic heterodyne sensor for rapid and**

- sensitive vapour detection.** *Nature Communications*, vol. 5, no. 1, pp. 1-7, July 2014.
10. M.W. Hoffmann, L. Mayrhofer, O. Casals, L. Caccamo, F. Hernandez-Ramirez, G. Lilienkamp, W. Daum, M. Moseler, A. Waag, H. Shen and J.D. Prades. **A highly selective and self-powered gas sensor via organic surface functionalization of p-Si/n-ZnO diodes.** *Advanced Materials*, vol. 26, no. 47, pp. 8017-8022, Dec 2014.
  11. L. Mai, L. Xu, Q. Gao, C. Han, B. Hu and Y. Pi. **Single  $\beta$ -AgVO<sub>3</sub> nanowire H<sub>2</sub>S Sensor.** *Nano Letters*, vol. 10, no. 7, pp. 2604–2608, July 2010.
  12. X. Pan, X. Liu, A. Bermak and Z. Fan. **Self-gating effect induced large performance improvement of ZnO nano-comb gas sensors.** *ACS Nano*, vol. 7, no. 10, pp. 9318–9324, Oct 2013.
  13. O., Alev, E., Sennik, N. Kilinc and Z. Z. Ozturk, **Gas Sensor Application of Hydrothermally Growth TiO<sub>2</sub> Nanorods.** *Procedia Engineering*, vol. 120, pp. 1162–1165, Jan 2015.
  14. J.R. Nataraj, P.Y. Bagali, M. Krishna and M.N. Vijayakumar. **Development of Silver Doped Titanium Oxide Thin films for Gas Sensor Applications.** *Materials Today: Proceedings*, vol. 5, no. 4, pp. 10670–10680, Jan 2018.
  15. A. M. Selman, and M. Husmam. **Calcination induced phase transformation of TiO<sub>2</sub> nanostructures and fabricated a Schottky diode as humidity sensor based on rutile phase.** *Sensing and Bio-Sensing Research*, vol. 11, pp. 8–13, Dec 2016.
  16. G. K. Mor, O. K. Varghese, M. Paulose, K. Shankar and C. A. Grimes. **A review on highly ordered, vertically oriented TiO<sub>2</sub> nanotube arrays: Fabrication, material properties, and solar energy applications.** *Solar Energy Materials and Solar Cells*, vol. 90, no. 14, pp. 2011–2075, Sep 2006.
  17. U. Diebold. **The surface science of titanium dioxide.** *Surface Science Reports*, vol. 48, no. 5–8, pp. 53–229, Jan 2003.
  18. H. Jeong, Y. Noh and D. Lee. **Highly stable and sensitive resistive flexible humidity sensors by means of roll-to-roll printed electrodes and flower-like TiO<sub>2</sub> nanostructures.** *Ceramics International*, vol. 45, no. 1, pp. 985–992, Jan 2019.
  19. S. M. Mokhtar. **Fabrication of titanium dioxide nanorods arrays for ultraviolet sensor application.** Doctoral dissertation, Universiti Tun Hussein Onn Malaysia, 2017.
  20. P. Singh, M. Abdullah, S. Sagadevan, C. Kaur and S. Ikram. **Highly sensitive ethanol sensor based on TiO<sub>2</sub> nanoparticles and its photocatalyst activity.** *Optik*, vol. 182, pp. 512-518, Apr 2019.
  21. M. Zhou, Y. Liu, B. Wu and X. Zhang. **Different crystalline phases of aligned TiO<sub>2</sub> nanowires and their ethanol gas sensing properties.** *Physica E: Low-Dimensional Systems and Nanostructures*, vol. 114, pp. 113601, Oct 2019.
  22. S. H. Salman, A. A. Shihab and A. H. K. Elttayef. **Design and construction of nanostructure TiO<sub>2</sub> thin film gas sensor prepared by RF magnetron sputtering technique.** *Energy Procedia*, vol. 157, pp. 283-289, Jan 2019.
  23. W. Yu, W. Zeng and Y. Li. **A nest-like TiO<sub>2</sub> nanostructures for excellent performance ethanol sensor.** *Materials Letters*, vol. 248, pp. 82–85, Aug 2019.
  24. L. Li, Z. Tong, W. Zhi-Jun, L. Shou-Chun, T. Yun-Xia and L. Wei. **High Performance Micro-Structure Sensor Based on TiO<sub>2</sub> Nanofibers for Ethanol Detection.** *Chinese Physic Letter*, vol. 26, no. 9, pp. 090701, Sep 2009.
  25. N.S. Khalid. **The effect of anatase on rutile TiO<sub>2</sub> nanoflowers towards its photo-catalytic activity on cancer cells,** Doctoral dissertation, Universiti Tun Hussein Onn Malaysia, 2016.
  26. A. Decroly, A. Krumpmann, M. Debliquy, D. Lahem, M. L. Larramendy and S. Soloneski. **Nanostructured TiO<sub>2</sub> layers for photovoltaic and gas sensing applications.** *Green Nanotechnology—Overview and Further Prospects*. InTech. Jun 2016.
  27. Y. Wang, L. Liu, C. Meng, Y. Zhou, Z. Gao, X. Li, X. Cao, L. Xu, and W. Zhu. **A novel ethanol gas sensor based on TiO<sub>2</sub>/Ag<sub>0.35</sub> V 2 O 5 branched nanoheterostructures.** *Scientific reports*, vol. 6, pp. 33092. Sep 2016.